Evidence for active ice retreat and ice-dammed lake formation during deglaciation in Raitts Burn

Emrys R. Phillips and Clive A. Auton

The Speyside area of the southern Monadhliath Mountains displays an exceptionally well-developed suite of landforms and deposits that formed during the latter stages of Late Devensian glaciation in this part of Scotland (Young, 1978; Hinxman and Anderson, 1915; Merritt *et al.*, this guide). This section of the field guide describes the glacial landforms and sediments present in the valley of Raitts Burn (NH 760 047 – 796 036). The burn flows south-eastwards across the north-western flank of Strathspey to join the valley of the River Spey c. 3 km downstream of Kingussie (Fig. 1). Exposed in the cliff sections cut by the burn is a sequence of rhythmically laminated clays, silts and sands, interbedded with ice-proximal diamictons and matrix-rich gravels (Auton 1998; Phillips and Auton, 2000). Detailed examination of the complex suite of sedimentary and glacitectonic structures developed within these sediments has revealed a complex sequence of depositional and deformational events recording the formation and overriding of an ice-dammed lake (Phillips and Auton, 2000). The glacial landform record in the area clearly indicates that this complex pattern of meltwater ponding and ice advance into the lake occurred in response to active ice retreat during the deglaciation of the Raitts Burn basin.

Quaternary geology of the Raitts Burn area

Raitts Burn drains an ice-scoured hollow (c. 1.5 km^2 across) cut into the resistant, mainly metasandstone bedrock of the Grampian Group. The overall pattern of streamlining of the bedrock in the area, as well as evidence of glacial scouring, plucking and striation, indicates a general SW to NE-direction of ice-movement (Fig. 1a) (Young 1978; Auton 1998). However, on the interfluve northeast of Craigbui Wood (Fig. 1b) glacial striae indicate a more SSW/NNE directed ice movement. Phillips and Auton (2000) suggested that this evidence may indicate either divergent flow within the ice sheet, governed by perturbations of the bedrock, when thick ice covered the whole area, or a later advance of a glacier ice onto the interfluve from the Spey Valley.

The landforms and sediments of the Raitts Burn area (Fig. 1) record the formation of an ice-dammed lake which was subsequently overridden by a minor readvance of the ice during an overall pattern of deglaciation. The former site of this small, ice-marginal lake is marked by a flat-lying area of boggy, peat covered ground to the west of the modern burn (Hinxman and Anderson, 1915; Auton, 1998). A suite of smooth, gently sloping benches (Fig. 1b) standing 10-15 m above the level of the floodplain of the burn were originally interpreted as deltas that prograded into this ice-marginal lake (Hinxman and Anderson, 1915). Although the morphology of the benches resembles gently sloping glaciofluvial terraces, or deltas, exposures in their frontal bluffs show that they are composed of weakly stratified, sandy diamicton. This diamicton can be seen to locally overlie a thin sequence of rhythmically laminated, glaciolacustrine silts and clays, resting upon a unit of poorly sorted matrix-rich boulder and cobble and pebble gravel. Consequently, the benches were considered by Phillips and Auton (2000) to be principally morainic, rather than deltaic, in origin. The six western benches (Fig. 1b) are dissected by arcuate glacial meltwater channels that grade to successively lower elevations southwards, recording successive still-stand positions of the ice margin as it retreated.

Stratigraphy and macroscale evidence of deformation

Representative lithological logs of the glacial deposits are shown in Fig. 1c. At location CA1035 the lower part of the sequence (Unit I) comprises a poorly stratified, clast-supported boulder and cobble gravel (2.8 m thick) resting directly on weathered Grampian Group metasandstone cut by granite sheets. The gravel comprises angular to subangular cobbles and boulders (> 40 cm in diameter) largely derived from the underlying bedrock, and possesses a hard, fine- to coarse-grained silty sand matrix. This coarse gravel is interpreted as an ice-proximal debris-flow or glaciofluvial fan deposit. At location CA1036 (Fig. 2a), Unit I is finer grained and contains more rounded metasandstone pebbles and cobbles, and therefore may represent a more distal part of the debris-flow which has undergone minor fluvial reworking. Phillips and Auton (2000) suggested that the Unit I gravels were laid down beyond an ice margin which had retreated northwards (towards the head of the valley of Raitts Burn) during the initial deglaciation of the area.

Unit I is overlain by a sequence of rhythmically laminated, graded, fine-grained glaciolacustrine sediments containing occasional thin interbeds of sand and sandy diamicton (Unit II). At location CA1035, Unit II comprises a 1 m thick sequence of upward-fining, sand-silt-clay rhythmites with 0.3-0.4 m thick sand interbeds occurring near the top and bottom of this succession. Sedimentary structures in the rhythmites include climbing-ripple lamination and small-scale water-escape (flame) structures. The sand beds are locally cut by steeply dipping, clay- and silt-lined fractures. A number of more thinly laminated sand beds in the middle of Unit II are boudinaged. Flame-structures developed in this part of the unit provide evidence of at least some soft-sediment deformation associated with localised liquefaction and water-escape. Some of the thicker sand beds have thin gravel lags, suggesting periods of more rapid water movement and sediment influx, perhaps associated with occasional drainage of the lake through or beneath its ice-dam. However, there is no evidence of desiccation or weathering indicating that subglacial drainage probably resulted in periodic lowering of the lake level rather than complete emergence and drying out of the lake sediments.

At location CA1036, the thinly laminated (silt-clay couplets typically 1-2 mm thick) rhythmites of Unit II are variably deformed with the intensity of faulting and folding increasing upwards through the sequence. The basal 0.5 m shows little macroscopic evidence of deformation with the lamination locally offset by small-scale, high-angle, NE-SW-trending normal faults. In the middle of the unit, the rhythmites are deformed by small-scale ENE-WSW-trending reverse faults (displacements of c. 20 cm) and folds which yield an overall N/NNW-directed sense of movement (Fig. 2b). The silt-clay couplets in this part of the unit also show evidence of fragmentation with the broken fragments forming discrete ‘rafts’ within a matrix of homogenous (fluidised) fine-sand, consistent with brittle deformation of the clays during the localised liquefaction of the sand in response to water-escape. In the upper part of Unit II, there is a marked increase in the intensity of deformation with the upper 0.1 m being deformed by small-scale, northerly-directed low-angle reverse faults (Fig. 2b) and gently inclined to recumbent, N/NNW-verging asymmetrical folds. Several of the fault planes, which cut through the fold hinges, are sub-parallel to the base of the overlying sandy diamicton (Unit III). At location CA1035, this stratified diamicton passes laterally into a clast-supported, poorly sorted, silty sandy gravel. At locality CA1036, Unit III is 11 m thick (Fig. 2a). The lower part of the diamicton is deformed by a number of small-scale, ENE-WSW-trending, low-angle reverse faults which are lined with laminated, normally graded fine-grained sand and silt. Unit III becomes more sandy and friable towards the top.

Micromorphology and microscale evidence of deformation

A detailed micromorphological and macro- and microstructural study of the deformation recorded by the glacially overridden glaciolacustrine deposits exposed at Raitts Burn has been published by Phillips and Auton (2000) (see also Phillips *et al.*, 2007, 2011) and is only summarised here. The polyphase deformation history recorded by the glaciolacustrine sediments comprises four phases (Phillips and Auton, 2000):

- Phase 1, initial loading/compaction of the sediments (pure shear) resulting in the imposition of a bedding-parallel throughout the rhythmites;
- Phase 2, heterogeneous deformation of this early fabric by kink bands and narrow ductile shears defined by a locally well-developed unistrial plasmic fabric;
- Phase 3, increasing pore water pressure within the lake sediments leading to soft-sediment deformation and localised liquefaction of the sands and silts, and formation of clay cutan and sand-filled hydrofractures; and
- Phase 4, subsequent folding and faulting within the uppermost part of the sequence.

This sequence was largely based upon the microstructures structures present within three orientated thin sections taken from the laminated clays and silts of Unit II at locality CA1036. However, the increase in the intensity and change in style of deformation upward through Unit II recorded by these thin sections can also be recognised on a macro-scale in the field.

The structurally lowest sample (S98555; Fig. 3) is relatively undeformed and comprises a sequence of finely laminated silts and clays cut by two, steeply inclined, clay-lined normal faults. These faults accommodated several phases of movement that resulted in localised drag folding and brecciation of the sediments in the immediate footwall and hanging-wall, with the clay lining recording the flow of water along these extensional structures. Thin (0.2-2.0 mm thick), normally graded, fine- to medium-grained sand laminae within the rhythmites records the periodic increase in clastic input into the lake. Scattered, coarse sand to small pebble-sized rock fragments (metasandstone, rhyolite) are interpreted as dropstones and are locally enclosed within distinct pressure shadows. The clay-rich laminae possess two planar plasmic fabrics: (1) a well-developed bedding-parallel S1 fabric developed during Phase 1 of the deformation history; and (2) a weaker, second (S2) fabric developed at approximately 15˚ to bedding (in the plane of section). S1 is locally deformed by a steeply inclined (80˚-90˚) set of lenticular to sigmoidal kink bands (NNW-directed sense of off-set) developed during Phase 2. Both bedding and the kink bands were later deformed by a set of reverse microfaults and small-scale shears.

Sample S98557 (Fig. 4), taken from the middle of Unit II, shows an increase in the intensity of soft-sediment deformation. A well-developed, bedding-parallel S1 fabric (Phase 1) present within the laminated clay and silt in the lower part of the thin section (A on Fig. 4) is deformed by at least one set of kink bands and small-scale shears (Phase 2). These fine-grained sediments are cut by a number of fractures filled by homogeneous fine-grained sand containing angular fragments of clay, broken from the side-walls. The sand filling these water-escape features (hydrofractures) was derived from an overlying, 10-15 mm thick sand bed (B on Fig. 4) which has been homogenised during liquefaction associated with water-escape during Phase 3 of the deformation history. This fluidised sand layer is overlain by silts and sands which possess a well-developed convolute lamination (C on Fig. 4). These laminated sediments are also cut by a number of sand-filled water-escape conduits and microfaults. The medium-grained sand in the upper part of the thin section is deformed by a complex reverse fault comprising an anastomosing network of discrete shear planes (dextral sense of movement) enclosing lenses of deformed laminated clay and silt (Fig. 4). Fine-scale shears within the clay lenses are defined by a very well-developed unistrial plasmic fabric. The lack of evidence for the injection of fluidised sand along the fault, coupled with it truncating the convolute laminated silts and sands (Fig. 4), clearly indicates that faulting

(Phase 4) post-dated soft-sediment deformation and liquefaction of the underlying sandy sediments.

Sample S98556 (Fig. 5) represents the most intensely glacitectonised upper part of Unit II. These highly deformed laminated clays and silts are overlain by a weakly stratified, apparently less intensely deformed diamicton (Unit III). A range of both ductile and brittle structures (Phase 4) are developed in the rhythmites including: upright to recumbent folds, discrete shear planes, thrusts, normal and reverse faults, as well as a locally intense planar to crenulation-style fabrics. Dark coloured laminae within the clay and silt provide useful marker horizons for unraveling the complex structure of this sample (see Fig. 5). Normal grading within the rhythmites shows that, in general, they are the right-way-up. However, localised overturning does occur on the short, steep limbs of recumbent folds. Analysis of sample S98556 by Phillips *et al.* (2011) revealed that the diamicton is deformed by a conjugate set of discontinuous clast microfabrics defined by lens-shaped microfabric domains (Fig. 5). The first of these fabrics, SDm1 (pale purple on Fig. 5), dips towards the NNW (i.e. down-ice) and occurs parallel to (in this plane of section) the stratification and layer-parallel plasmic fabric present within the diamicton. Both SDm1 and layer-parallel plasmic fabric wrap around the larger lithic clasts, with the asymmetry of these fabrics recording a NNW-directed sense of shear. SDm1 is also coplanar to the ductile shears and normal faults (rose diagrams on Fig. 5) present within the underlying rhythmites (Unit II). The second, more pervasively developed SDm2 clast microfabric (blue on Fig. 5) within the diamicton dips towards the SSE (i.e. up-ice) and occurs parallel to a heterogeneously developed unistrial plasmic fabric defining a set of closely spaced ductile shears (dextral off-set) within the matrix (rose diagrams on Fig. 5). This relationship suggests that both SDm2 and shears were imposed simultaneously, defining a 10-12 mm wide zone of enhanced ductile shear (green area on Fig. 5) with an overall sense of displacement towards the NNW. This zone clearly offsets the contact between the diamicton and rhythmites, and can be traced into the underlying laminated sediments where it occurs parallel to a set of well-developed (Phase 4) reverse faults (Fig. 5).

Origin of rhythmic lamination within the glaciolacustrine sediments

The systematic fluctuations in grain size and thickness identified within the rhythmically laminated sediments in Unit II (Fig. 3) are indicative of cyclic variations in sediment supply. Such fluctuations may result from daily, meteorological or annual variations in sediment discharge into lakes (Church and Gilbert, 1975). Short-term (daily/meteorological) cycles typically produce thin, macroscopically normally graded laminae with sharp basal contacts, forming gradational fining-upward units. In contrast, annual cycles tend to produce distinct silt-clay couplets (varves) with macroscopically planar, sharp contacts between coarse- and fine-grained components. These result from marked differences in sediment supply between summer and winter (De Geer, 1912; Ashley, 1975; Smith, 1978; Benn and Evans, 2010). Phillips and Auton (2000) concluded that the macroscopically planar, sharp contacts between the silt and clay couplets in sample S98555, suggest that these lacustrine sediments are true annual varves.

Analysis of the varves in thin section S98555 (which have only suffered minor post-depositional disturbance) indicates an approximate frequency of 50 varves within 10 cm of rhythmically laminated sediment (Fig. 3). Using this frequency as representative of the sequence as a whole, then 1.2 m of varved sediment preserved at location CA 1036 may equate to c. 600 years of glaciolacustrine deposition. This simplistic figure is probably an underestimate, however, as depositional hiatuses (caused by erosion during periods more rapid water movement, associated partial drainage of the lake) are present in the sequence and its upper surface is truncated by the overlying diamicton.

Deformation of the glaciolacustrine sediments associated with glacier advance

Phillips and Auton (2000) concluded that the orientation and kinematics recorded by all the macro- and microstructures present within both the diamicton (Unit II) and underlying glaciolacustrine sediments (Unit III) are consistent with their formation in response to the same stress regime and that the intensity of this deformation increased with time (see also Phillips *et al.*, 2007, 2011). The deformation sequence outlined above can be directly applied to modelling the glacial and deglacial events within the Raitts Burn basin which followed initial regional ice-sheet decay. The progressive deformation of these sediments can be explained in terms of ice advance across the lake basin towards the NNW (Phillips and Auton, 2000). The observed differences in the style and apparent intensity of deformation displayed by the deposits can be directly related to the contrasting lithology and potentially much higher pore-water content and/or pressure occurring within the diamicton during subglacial deformation.

All of the glaciotectonic structures in Unit II and the lower parts of Unit III relate to the advance of ice northwards across the lake basin. The earliest phase of this deformation (Phase 1), which led to the imposition of a bedding-parallel throughout the rhythmites, accompanied the initial loading of the lake sediments by the overriding ice. Continued advance of the glacier into the lake resulted in heterogeneous deformation of this early fabric by kink bands and narrow ductile shears (Phase 2), followed by soft-sediment deformation and localised liquefaction of the sands and silts (Phase 3) due to an increase in pore water pressure within the rhythmites. Subsequent folding and faulting (Phase 4) within the uppermost part of the sequence resulting from shear imposed by the overriding ice. The undeformed sandy diamictons which form the upper parts of Unit III, are interpreted as ice-contact, subaerial debris-flows that have undergone a degree of winnowing and sorting by meltwater at an ice margin. These deposits represent the morainic material laid down at the front of the ice as it retreated.

Phillips and Auton (2000) concluded that, morphologically, the Raitts Burn morainic benches resemble composite ridges and thrust block moraines (Evans, 1991; Benn and Evans, 2010) separated by arcuate glacial drainage channels (Fig. 1). The arcuate shape of the benches and the decline in their elevation south-westwards on the western side of the burn led Phillips and Auton (2000) to argue for a south-westerly retreat of the ice-front in this area. In contrast, the slopes of the eastern benches, which occur within an arc between NE and SE, record a pivoting and splitting apart of eastern flank of the ice front during retreat. This model of glacial advance and retreat is probably also applicable to the nearby valleys of Glen Gynack and Allt na Baranachd, where similar morainic sediments are preserved. Establishing patterns of meltwater ponding, ice advance and retreat at critical sites, such as Raitts Burn, has the potential to elucidate the complex local variations in the regional pattern of deglaciation in the Central Highlands of Scotland towards the end of the main Late Devensian glacial episode.

References

Ashley, G.M. 1975. Rhythmic sedimentation in glacial Lake Hitchcock, Massachusetts-Connecticut. In Joping, A.V., McDonald, B.C. (eds.) *Glaciofluvial and Glaciolacustrine Sedimentation*. SEPM, Special Publication. **23**, 304-320.

Auton, C.A. 1998. Aspects of the Quaternary Geology of 1:50,000 Sheet 74W (Tomatin). British Geological Survey, Technical Report. **WA/98/21**.

Benn, D.I., Evans, D.J.A. 2010: Glaciers and Glaciation. 802 pp. Arnold, London.

Church, M., Gilbert, R. 1975. Proglacial fluvial and lacustrine sediments. In Joping, A.V., McDonald, B.C. (eds.) *Glaciofluvial and Glaciolacustrine Sedimentation*. SEPM, Special Publication **23**, 22-100.
De Geer, G. 1912. A geochronology of the last 12,000 years. 11th International Geological Congress, Stockholm. *Compte. Rendu*. **1**, 241-258.
Evans, D.J.A. 1991. Canadian Landform Examples - 19: High Arctic thrust block moraines. The *Canadian Geographer*. **35**, 93-97.
Hinxman, L.W., Anderson, E.N. 1915. *The geology of mid-Strathspey and Strathdearn, explanation of Sheet 74*. Memoir of the Geological Survey, Scotland.
Phillips, E.R., Auton, C.A. 2000. Micromorphological evidence for polyphase deformation of glaciolacustrine sediments from Strathspey, Scotland. In Maltman, A.J., Hubbard, B., Hambrey, M.J. (eds.) *Deformation of glacial materials*. The Geological Society of London. Special Publication No. **176,** 279-291.
Phillips, E.R., Merritt, J.W., Auton, C.A., Golledge, N.R. 2007. Microstructures developed in subglacially and proglacially deformed sediments: faults, folds and fabrics, and the influence of water on the style of deformation. *Quaternary Science Reviews*. **26**, 1499-1528.
Phillips, E.R., van der Meer, J.J.M., Ferguson, A. 2011. A new 'microstructural mapping' methodology for the identification and analysis of microfabrics within glacial sediments. *Quaternary Science Reviews*. **30**, 2570-2596.
Young, J.A.T. 1978. The landforms of the Upper Strathspey. *Scottish Geographical Magazine*. **94**, 76-94.

Figures

Fig. 1. (a) Location of the Raitts Burn study area, Strathspey, Scotland. (b) Simplified geological map of the Quaternary deposits and landforms in the Raitts Burn area.(c). Simplified lithological logs for the Quaternary deposits exposed at locations CA1035 and CA1306, Raitts Burn.

Fig. 2. (a) River cliff at Locality CA 1036, Raitts Burn, showing the 3 lithological units. (b) Small-scale reverse faults cutting silt-clay rhythmites, top of Unit II showing sense of movement towards NNW.

Fig. 3. Microstructural map of sample S98555 (see text for details).

Fig. 4. Microstructural map of sample S98557 (see text for details) showing the relationships between earlier developed soft-sediment deformation structures associated with water-escape, and shearing associated with the prominent later reverse fault. Area A - laminated clay and silt; Area B – fluidised sand containing rafts of laminated clay and silt derived from A; and area C - laminated fine sand and silt deformed by soft-sediment deformation structures.

Fig. 5. Microstructural map of sample S98556 (see text for details) showing polydeformed, thinly laminated sand silt and clay (Unit II) overlain by diamicton (Unit III) (after Phillips et al., 2011).

a

Raitts Burn

study area

Kingussie

River Spey

Strathspey

River Truim

1 km

N

b

0 metres 500

N

CA1035

CA1036

Raitts Burn

Craigbui Wood

Creag Bheag

78

03

79

04

regional ice movement direction

bedrock at or near surface

subglacial till

proglacial deposits (sandy diamicton)

rhythmites (sand, slit and clay)

boulder fan (glaciofluvial)

peat

sandy alluvium

river terrace (gravel)

glacial striations

logged section

slope of bench

glacial drainage channel

c

metres

0

2

4

6

8

10

12

S98556

S98557

S98555

Description/interpretation

Unit III: clast-supported sandy diamicton, passing laterally into poorly sorted matrix-rich gravel
Glacigenic deposit

Unit II: sand-silt-clay rhythmites, minor interbedded diamictons and sands
Over-ridden glaciolacustrine deposits

Unit I: matrix-rich, clast-supported boulder and cobble gravel
Proglacial debris flow deposit

location CA1036
[NH 7821 0362]

location CA1035
[NH 7798 0418]

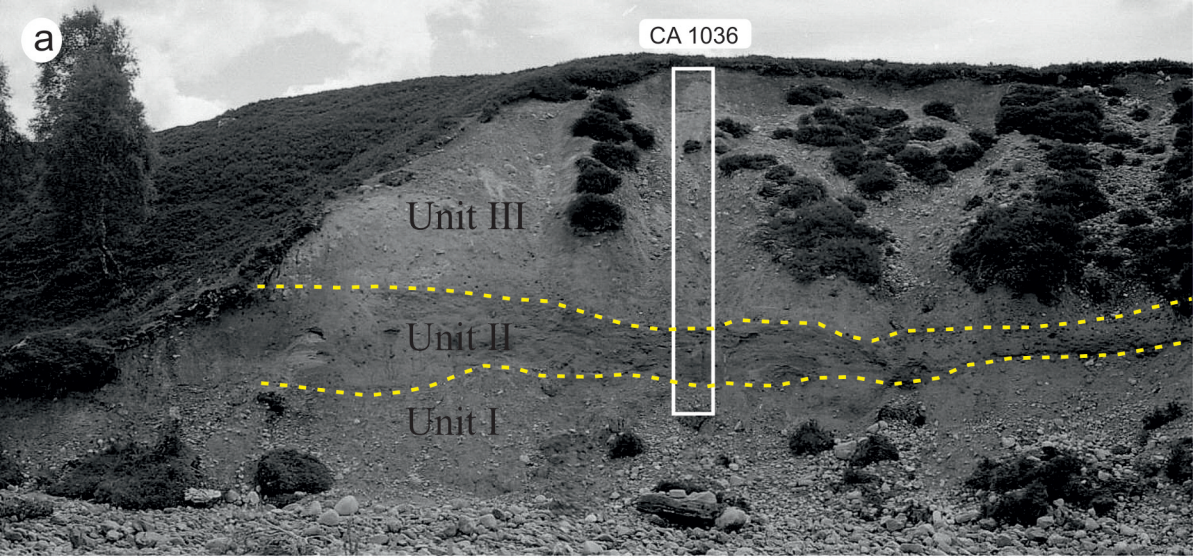

Sense of movement on low-angle reverse faults (thrusts)

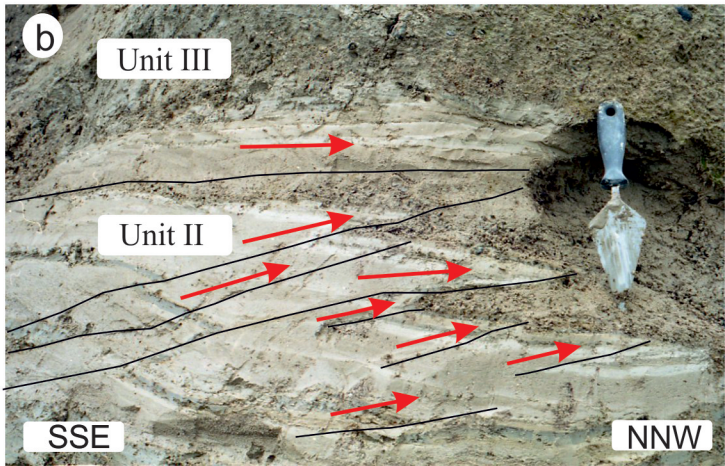

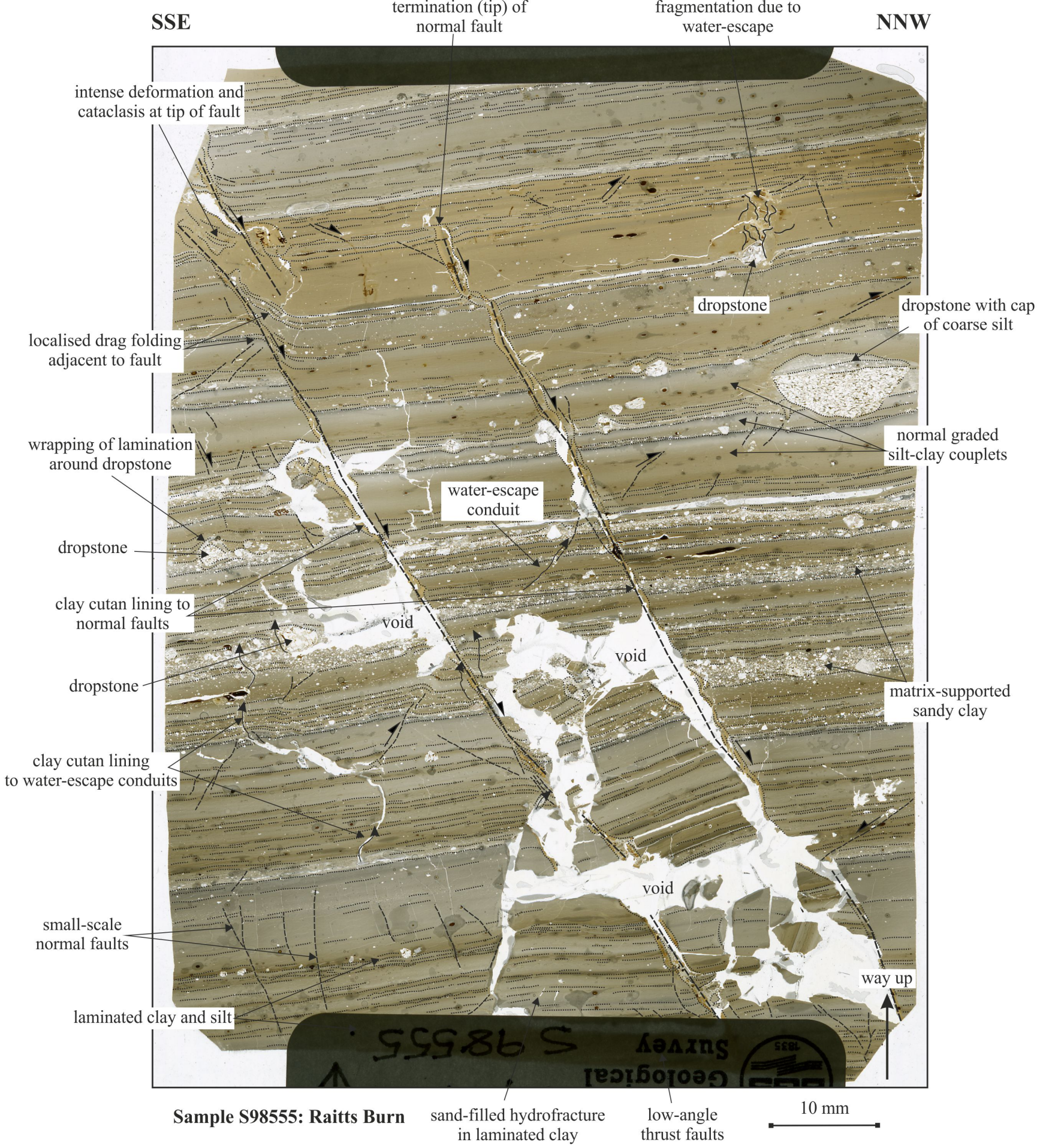
SSE
termination (tip) of normal fault
fragmentation due to water-escape
NNW
intense deformation and cataclasis at tip of fault
dropstone
dropstone with cap of coarse silt
localised drag folding adjacent to fault
normal graded silt-clay couplets
wrapping of lamination around dropstone
water-escape conduit
dropstone
clay cutan lining to normal faults
void
void
dropstone
matrix-supported sandy clay
clay cutan lining to water-escape conduits
void
small-scale normal faults
way up
laminated clay and silt
Geological Survey
S 98555
Sample S98555: Raitts Burn
sand-filled hydrofracture in laminated clay
low-angle thrust faults
10 mm
sense of displacement on faults
faults

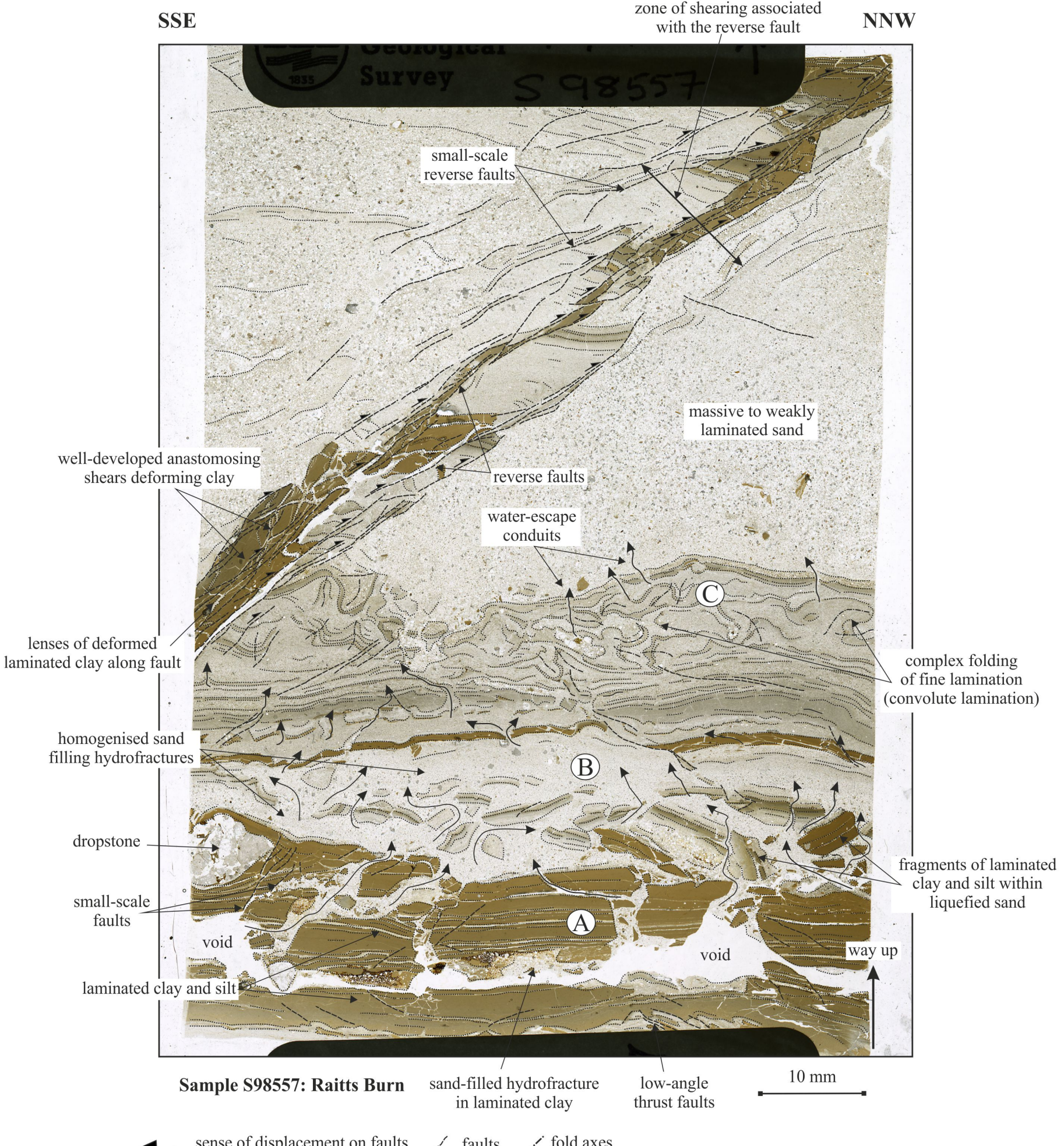
SSE
NNW
zone of shearing associated with the reverse fault
small-scale reverse faults
massive to weakly laminated sand
well-developed anastomosing shears deforming clay
reverse faults
water-escape conduits
C
lenses of deformed laminated clay along fault
complex folding of fine lamination (convolute lamination)
homogenised sand filling hydrofractures
B
dropstone
fragments of laminated clay and silt within liquefied sand
small-scale faults
A
void
void
way up
laminated clay and silt
Sample S98557: Raitts Burn
sand-filled hydrofracture in laminated clay
low-angle thrust faults
10 mm
sense of displacement on faults
faults
fold axes

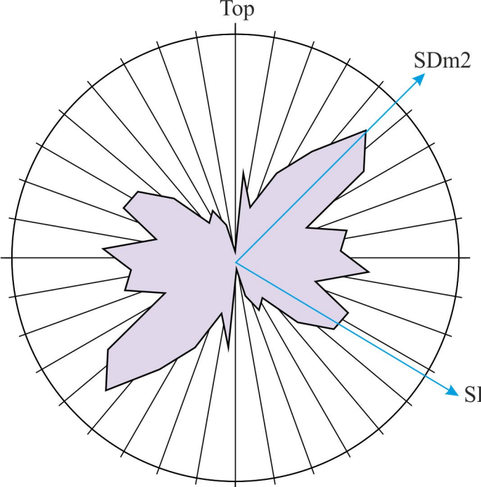

sample S98556: clast microfabrics (N = 371)

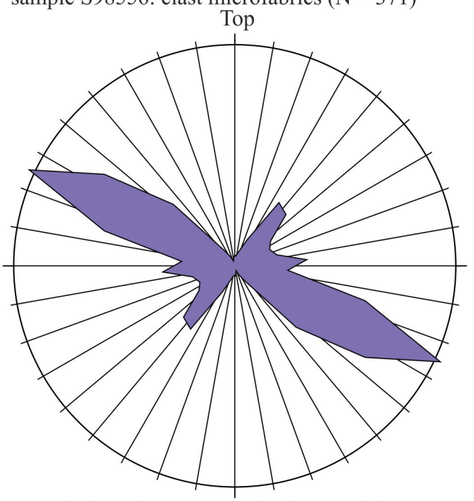

sample S98556: unistrial plasmic fabric/shears (N = 229)

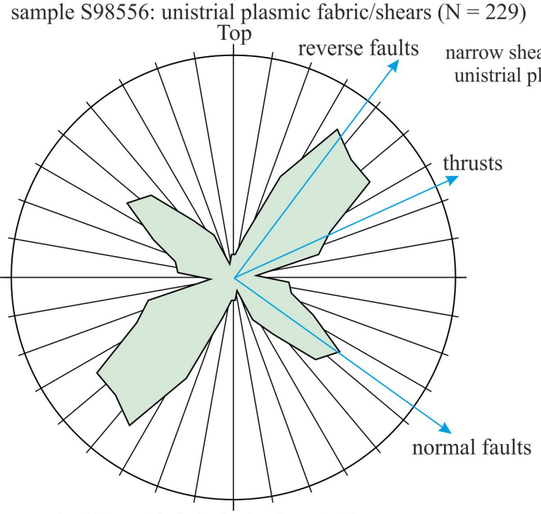

sample S98556: brittle faults (N = 326)

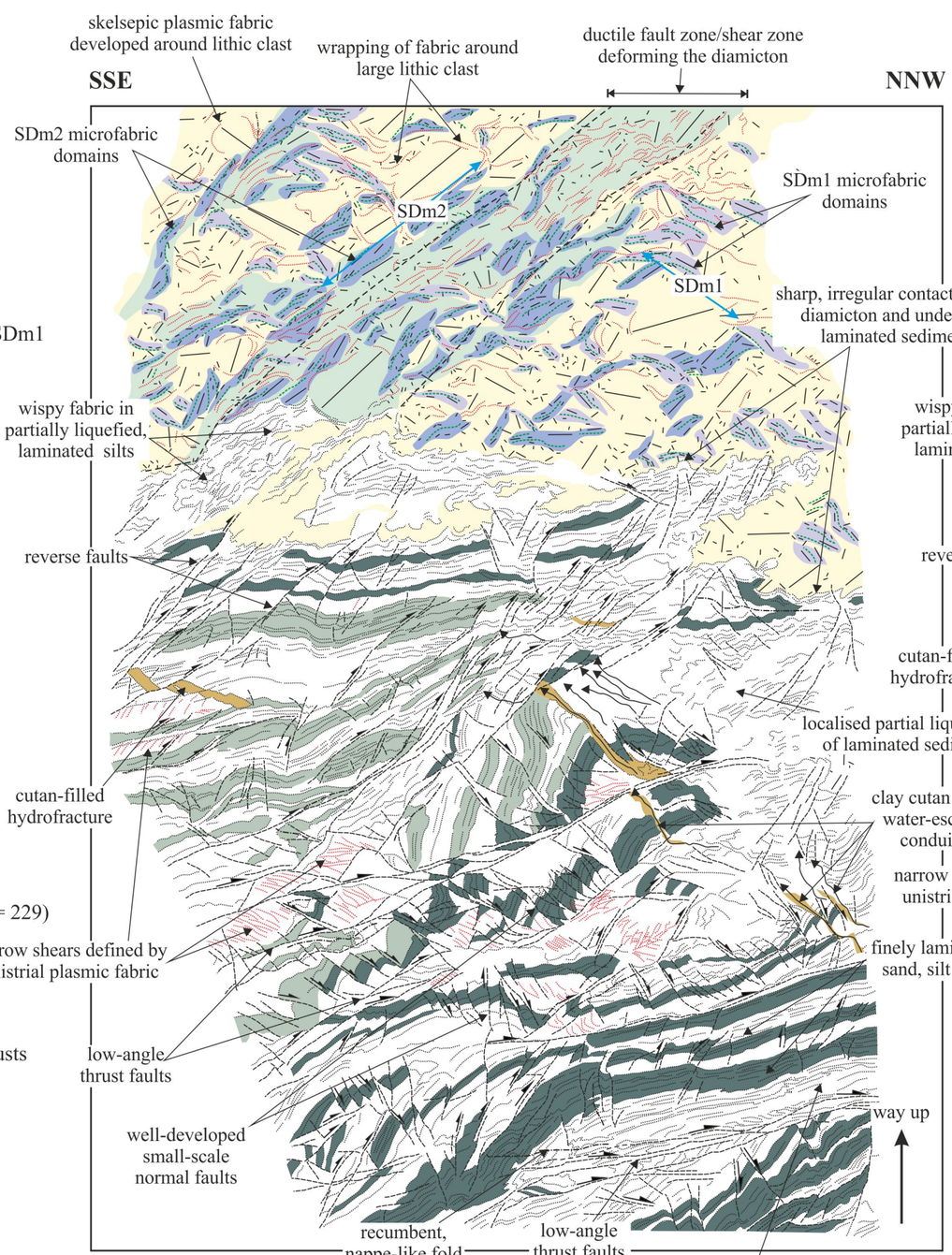

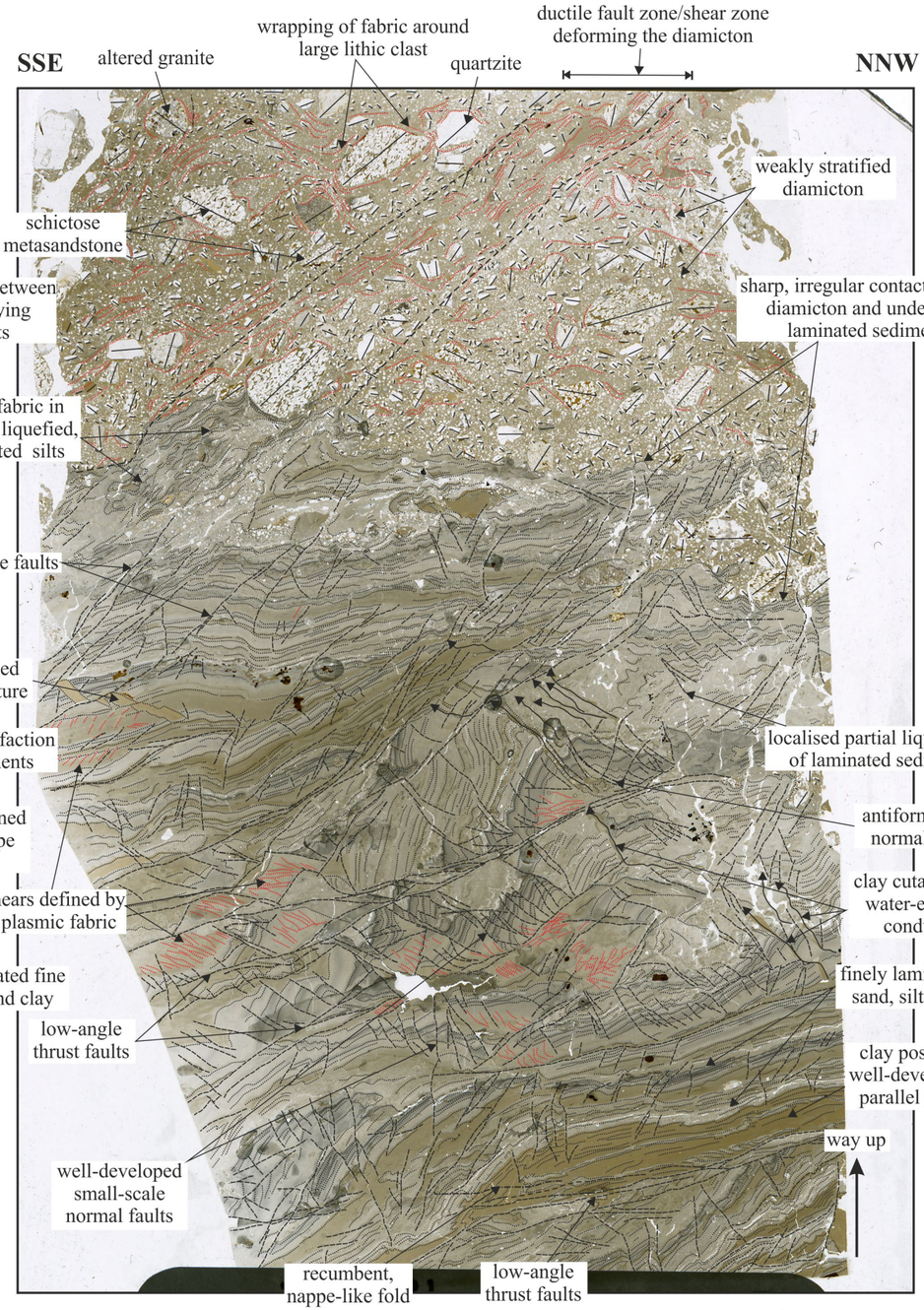

Sample S98556: Raitts Burn

axial surfaces of crenulations/microfolds

plasmic fabrics and grain alignments

trace of folds deforming bedding

microclast fabric defined by clast long axes

orientation of fabric(s) SDm1 to n relative age of fabric(s)

sense of displacement on faults faults long axis of clasts